Chapter 4

Modeling the macrostructure of the heart as a dynamic double helical band

4.1 Introduction

Importance of heart modeling hardly needs a justification – it is widely accepted. However, it is less widely recognized how simple and yet profound are some of the questions in the field which remain either completely open or incompletely understood. Here, we will focus on two such questions: First, we consider the ability of the heart to produce large ventricular cavity volume changes with only small local cellular deformations. And second, we look at the principles behind the heart's intricate dynamical behavior in terms of changing twist of the left ventricle during each heartbeat. Let us comment in more details on these two aspects and their relation to each other.

On the one hand, the active components of the myocardium mass – the myocyte cells – deform by a relatively small amount, with maximum contraction ratio of only 15% [16]. On the other hand, the left ventricular volume exchange ratios, known as ejection fractions, are normally above 55%. Thus, the volume of the internal chamber of the heart decreases by more than half its diastolic value, while each cell contracts by less than a sixth length-wise. Geometrically this would be impossible to achieve without wall thickening effects or helical fibers. In the present chapter, we will concentrate on the latter, because the helical arrangement of the fibers is responsible for the twisting-untwisting of the heart with its beating cycles [55].

In the beating heart, the changes in these two geometrical aspects of cardiac behavior, volume and twist, are intricately coordinated. Indeed, in their ground breaking imaging studies that involved surgically placing markers on the heart Beyar, [29] and Miller [27, 28] were able to provide first accurate measurements of the left ventricle's twist. Based on these measurements, they hypothesized that the sensitive timing relationship between the twist of the left ventricle and the volume exchange

dynamics is an important aspect of the heart's volume efficiency. This hypothesis has received further confirmation with investigators taking advantage of the improvements in speckle-tracking imaging [30, 33] and MRI techniques [32], showing that the relationship between ejection fraction and twist changes differently with age and various heart diseases. The characterization of this timing relationship could lead to innovative diagnostic procedures [64]. In the present chapter, we aim to understand and model the well orchestrated correlation between twist and volume exchange.

The nature of the questions which we want to address implies that we should employ a fairly simple model which only captures the very basic features of heart geometry and dynamics. This will allow us to understand to which extent the twist-volume exchange timing is a reliably generic property which could give rise to a diagnostic technique. In general, heart modeling attracted a lot of efforts over the years (see [16] and references therein), and some of the models examined were beautifully simple. One of these models constructed by Sallin [41] explored the need for helical fiber architecture in order to achieve physiological ejection fractions . Another simple left ventricle membrane model, by Needleman et al. [65], explored the difference for normal and infarcted left ventricle in the important pressure volume relationship of the cardiac cycle. An alternative approach, time-varying elastance model, characterized the pumping function of the heart [66]. Sunagawa and Sagawa also gave the most useful summary and comparison of models developed at the time [66].

The most popular current cardiac models simulate the myocardium as a series of shells with differently directed helical fibers [16, 35, 44]. This type of model is based on histological images taken by Streeter in 1969 [20], which show that there is a gradual change in the direction of the fibers with the epicardium and endocardium fibers directed axially, while the fibers in the middle are directed circumferentially. These models have been greatly advanced by the McCulloch group through the development of the constitutive relations for the myocardium materials based on the three dimensional strain measurements [47, 48, 51]. The computational approaches based on finite element models are capable of exploring such issues as optimization of fiber architecture [45], performance of normal and dilated failing hearts when the finite element model included electro-mechanics [53, 54], and a combination of the circulatory system with the ventricular models [52]. Other finite element models explore ischemic left ventricles [67] and arrythmia [46]. Yet another type of models developed by Peskin et al. uses the immersed boundary method [42, 43]. These current models rarely achieve physiological ejection fractions while observing the limit of 15% fiber contraction. A notable exception is a "one fiber" model developed by Arts et al. [68, 69]. The idea of a "one fiber" model based on the work of both Streeter [20], mentioned previously, and Torrent-Guasp [21], which we describe below. However, none of these modeling works touched upon the important relationship between the twist of the left ventricle and the ejection fraction.

In our approach, we will build our model based on the idea of a single helical band representing the dominant structure in the heart. This idea was originally proposed by Torrent-Guasp [21] alongside

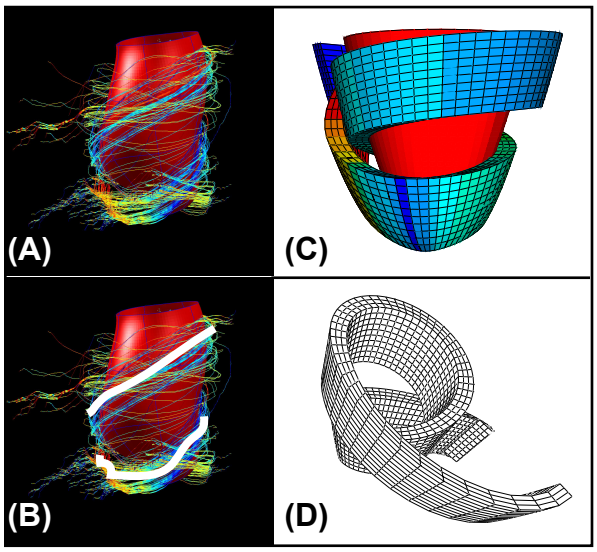

Figure 4.1: (A)Figure of muscle fiber DTMRI provided to us by Helm; (B)The DTMRI image of the muscle fibers overlayed with the major band direction; (C) The simplified band color coded with the direction of the fibers in the same manner as the DTMRI images; (D) The simplified band with no color coding.

Streeter's fundamental work [20]. Torrent-Guasp postulated that the heart muscle fibers form a helical single band that starts from the pulmonary aorta, hugs the right ventricle, winds down to the apex as the descending segment, and then spirals up to the aortic valve as the ascending segment [21]. Recent advancements in MRI technology, specifically the DTMRI technique, enable us to create isolated images of the myocyte fibers, instead of a combination of muscle and collagen fibers [23]. Images obtained using this technology provide further credence to the representation of the heart as a helical band (figure 4.1).

The similarities between the heart myocardium fiber structure and the double helix band give rise to a simplified model, one that allows simulation of more complicated excitation patterns and the dynamic response. It is worth our while to evaluate this simplified model as the dominant structure because it gives us an opportunity to isolate the macrostructure responsible for the behavior of the heart. The excitation patterns are picked so the double helix band model produces the same ejection fraction characteristics as a physiological left ventricle. The full dynamic model is then validated by comparing its twist behavior with the twist of an actual heart over one beat.

4.2 Methods

To give a framework for the structure of the myocardium we assume that the macrostructure of the muscle fibers takes the form of the double helical band described earlier. To simplify the model we assume the band to have a constant width (seen in figure 4.1D). The first necessary step then is to

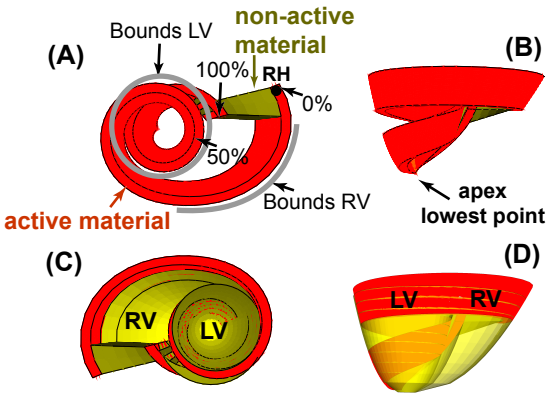

Figure 4.2: Initial shape of the double helical model. The active material is shown in red, the non-active material is shown in dark green, and the fitted chamber surfaces are shown in transparent yellow. (A) The band is shown from the top. The grey lines indicate the portion of the band that bounds the right and left ventricles. The coordinate system used to specify the excitation pattern is specified, with zero at the pulmonary aorta start of right heart (RH), and 100 at the opposite end of the band. (B) The side view of the band, with the apex indicated at the lowest point. (C) Top view with the fitted volumes for left ventricles (LV) and right ventricle (RV) labeled on the pictures. (D) Side view with the ventricles labeled the same way as in (C).

formulate mathematical description of this rather complex three dimensional object. To do that, we first consider an axis line of the band that follows in the direction of fibers through the center of the proposed shape. The next step is to expand the line into a strip with both a width and a thickness. Notice, that with this approach the tangent direction of the centerline is, by construction, the same as the direction of the muscle fibers. The following is the equation of the centerline of such a strip in cylindrical coordinates, where θ ranges from zero to slightly over 4π. Factor 1 is responsible for separating the band at the cross-over point, and Factor 2 regulates the size of the right ventricle. The values of the constants were taken to be such that the resulting shape matched the size of an average human heart: $C_1 = 4.9$ cm, $C_2 = 7$ cm, $A_1 = 1.3$, $A_2 = 0.5$, $C_3 = -0.77$ cm, $C_4 = 1/6$ and $C_5 = 1$.

$$\begin{aligned} z_{cent} &= C_1 - C_2 \frac{\theta^{A_1}}{A_2} \exp\left[-\frac{\theta}{B_2}\right], \\ r_{cent} &= \sqrt{z_{cent} + C_3}\left[1 + C_4 \cos\left(\frac{\theta - \theta_{crossing}}{2}\right)\right] \\ &\quad \left[1 + C_5 \exp\left(-(\theta - \theta_{right})^2\right)\right] \\ &= \sqrt{z_{cent} + C_3}\,[\text{Factor 1}]\,[\text{Factor 2}]\,. \end{aligned} \tag{4.1}$$

Once the centerline of the band is fixed, the band itself can be built about this line:

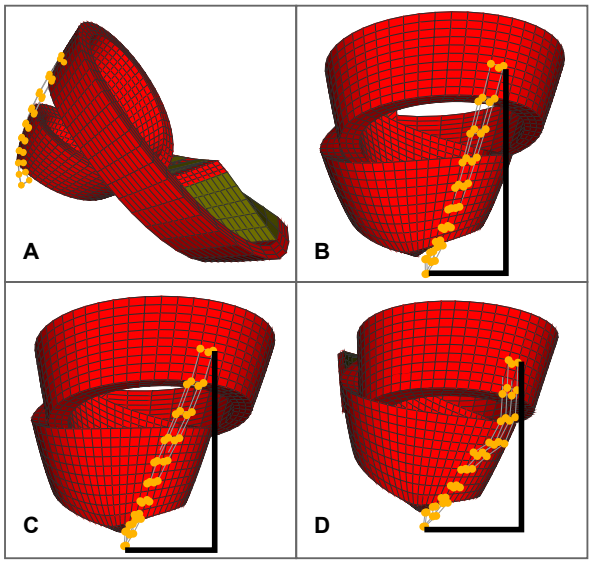

Figure 4.3: The double helical band with the twist markers. The band is indicated in red, the markers are yellow circles connected with grey lines. The thick black lines are drawn for assist visual estimates of out of plane deformation. (A) The relaxed band model with the markers used to calculate twist shown from the side; (B) The relaxed band with the marker shown from the back; (C) The markers shown for a band that has started to contract – notice that there is already an out of plane deformation. (D) The markers shown at end-systole – notice that the elastic material with the markers has buckled in plane as well as twisted out of plane.

$$\begin{aligned} z &= z_{cent} + \xi \\ r &= \sqrt{z_{cent} + C_3}\,[\text{Factor 1}]\,[\text{Factor 2}] + \zeta \\ x &= r\cos\theta \qquad y = r\sin\theta, \end{aligned} \tag{4.2}$$

where ξ regulates the width of the band and ζ regulates its thickness.

To close the loop, the ends of the band are connected with a non-active material, like collagen, which is not subject to excitation-induced active contraction. A piece of the same material is also used to keep the band together at the cross-over point. The band bounds both the left and right ventricle as shown in figure 4.2A. The volumes were calculated by virtually extending the muscle band to create an enclosed space (figure 4.2C and 4.2D). The left and the right ventricles of the heart were modeled as a paraboloid and a half-paraboloid, respectively.

To calculate the twist, it was necessary to mimic the measuring techniques used in experimental studies where markers are placed along one side of the left ventricle and their positions recorded. In our model, the initial position of the markers was in a vertical plane, on a single parabola on the side of the left ventricle (figure 4.3A and 4.3B). As the band contracted, this parabola was distorted as shown in figure 4.3C and 4.3D.

In a physiological study, the twist is calculated by plotting the degree of rotation at each marker

against their long axial positions and estimating the slope. The computational counterpart of this procedure can be implemented as follows. During the deformation of the band the set of markers can deform in the vertical plane or out of this plane. When the long axis of the left ventricle shortens during contraction the set of indicator markers deform in plane. In the shortening of the long-axis the top and bottom portions of the left ventricle band come closer together, and to accommodate this deformation the strip with the markers buckles outwards. However, unless the top and bottom portions of the band rotate with respect to each other, the buckling will occur in the same vertical plane. Conversely, in twisting of the left ventricle the bottom and top portions of the band move with respect to each other in the horizontal plane. As a result the set of markers deform out of the vertical plane. The greater the twist of the left ventricle, the greater is this out of plane deformation. To calculate the value of the twist, we directly relate it to the out of vertical plane deformation of the set of twist markers. The magnitude of the out-of-plane movement, d, was calculated from knowing the position of the markers, and the twist was then given by:

$$\text{twist} = -\frac{3\sqrt{3}}{2}\frac{d}{(\text{LA})(\text{r}_{\text{top point}})}, \tag{4.3}$$

where, LA and $r_{\text{top point}}$ are the long axis length and the radial position of the top point, respectively. This relation between d and twist is easily derived by assuming that a paraboloid shell is twisted such that the rotation angle around z-axis is linearly dependent on z. For ease of visualization the markers are made to be a part of a soft strip of material, a "twist indicator." The material is three orders of magnitude softer than the material of the band, and thus does not impact the deformation of the band.

For the model examined in the present chapter, we assumed that the double helical band remains in elastic equilibrium at all times. This assumption is motivated by the fact that the forces developed in the muscle fibers are much greater than the resistance of the collagen network and blood pressure. To facilitate the complex task of computing elastic equilibrium in the highly non-trivial geometries of the dynamically evolving fiber shape, we adopt a software package: ABAQUS 6.5 Standard and its nonlinear static analysis. The output was analyzed using the ABAQUS 6.5 CAE in combination with Fortran and Matlab code. The contraction is modeled by providing a material characteristic of an expansion coefficient, so, when fully excited, the element can contract up to 15% in the direction of the fibers. Conservation of volume of the material is enforced by specifying appropriate expansion in the two perpendicular directions in response to the excitation. The excitation coefficient is specified to vary throughout the band with time, allowing for time dependent contraction waves.

To describe the intensity of excitation and its spatio-temporary pattern, we define a unitless quantity, which we simply call Excitation(x, t). We imagine that the fiber, at every point x at time t, contracts proportionally to the value of Excitation(x, t) such that when Excitation equals

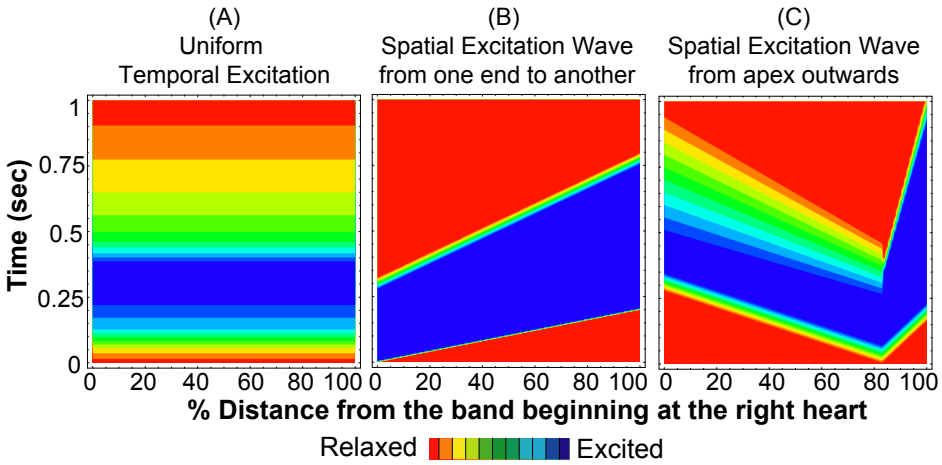

Figure 4.4: The contour plots show the degree of activation for each of the dynamic excitation schemed tried. From left to right it shows, (A) uniform temporal excitation, (B) a spatial excitation wave from one end of the band to the other, and (C) a spatial excitation wave starting at the apex. Below is the legend indicating that the red color represents the relaxed muscle fiber, while blue represents fully excited.

to -1 the element gets fully contracted, by 15% of its length. Therefore, the strain of the element due to excitation is given by $\varepsilon = 0.15 \times [\text{Excitation}(\text{x}, \text{t})]$. A series of different excitation waves were simulated, including a step wave (uniform excitation), a time dependent uniform excitation, and traveling waves of various shapes, including a spatial wave that follows the Purkinje excitation pattern [15], which has the contraction wave start at the apex and move outward and upward. For excitation schemes that are not spatial waves, the excitation value was simply specified to match roughly the desired ejection fraction evolution with time (figure 4.4A). A spatial wave excitation scheme is interpolated by the piece-wise linear profile:

$$\text{Excitation}(x,t) \quad = \quad \begin{cases} 0 & \text{at} \quad t < t_1 \\ -(t-t_1)/(t_2-t_1) & \text{at} \quad t_1 \le t < t_2 \\ -1 & \text{at} \quad t_2 \le t < t_3 \\ -(t_4-t)/(t_4-t_3) & \text{at} \quad t_3 \le t < t_4 \\ 0 & \text{at} \quad t \ge t_4 \end{cases} \tag{4.4}$$

where x is the coordinate on the band, starting from the beginning of the band at the right heart's pulmonary aorta (labeled RH in figure 4.2A), and t is time, and $t_1,\ t_2,\ t_3,\ t_4$ are specific to each contraction scheme. For a simple excitation scheme in which the excitation starts at the pulmonary aorta end of the band, and travels first through the right ventricle, and then through the left one, these are given by:

$$t_i = \frac{U_i}{L_{tot}} x + T_i, \tag{4.5}$$

where $i = 1, 2, 3, 4$, L_{tot} is the total length of the band, and U_i/L_{tot} is the inverse of the speed of the wave front. The parameters are $U_1 = U_2 = 0.2$ s, $U_3 = U_4 = 0.475$ s, $T_1 = 0$ s, $T_2 = 0.005$ s, $T_3 = 0.275$ s, $T_4 = 0.325$ s. For the excitation pattern that starts at the apex and moves outwards the equations become more complex:

$$t_i = \begin{cases} \frac{U_i^R}{\text{AI}}(\text{AI} - x) + T_i^R & \text{at} \quad 0 \leq x < \text{AI} \\ \frac{U_i^L}{L_{tot} - \text{AI}}(x - \text{AI}) + T_i^L & \text{at} \quad \text{AI} \leq x < L_{tot} \end{cases} \tag{4.6}$$

where $AI = 0.85 L_{tot}$ is the position of the apex (figure 4.2B), L_{tot} is the total length of the band, and U_i^R/AI and $U_i^L/(L_{tot} - \text{AI})$ are the inverse wave front velocities moving towards the right (pulmonary aorta) and left sides, respectively. The parameter values are: $U_1^R = U_2^R = 0.275$ s, $U_3^R = 0.225$ s, $U_4^R = 1.0$ s, $U_1^L = U_2^L = 0.15$ s, $U_3^L = 0.55$ s, $U_4^L = 0.625$ s, $T_1^R = T_1^L = 0$ s, $T_2^R = T_2^L = 0.075$ s, $T_3^R = 0.25$ s, $T_4^R = 0.475$ s, $T_3^L = 0.325$ s, $T_4^L = 0.375$ s. The contour plots of the excitation pattern for the wave forms used in this chapter are shown in figure 4.4. For this Purkinje type spatial wave the point where the excitation and relaxation fronts start can be moved by changing the value of the constant AI.

4.3 Results and Discussion

4.3.1 Large volume changes – small local deformations

The first step in assessing the validity of the double helical macrostructure model is to track the volume changes in the left ventricle. Figures 4.5A and 4.5B show the band at diastole (initial configuration) and systole (most contracted) for different excitation patterns, respectively. The snapshots demonstrate qualitatively how the volume of the left ventricle is reduced.

To quantify the left ventricular pumping ability, the ejection fraction is calculated. Figure 4.6 shows the plot of the ejection fraction vs. time for three sample excitation schemes along with idealized physiological data. The double helical myocardial model provides physiological ejection fractions of over 55% for any type of excitation wave. It is worth emphasizing that this is achieved without forcing the myofibrils in excess of their physiological contractile ability and without optimization of the temporal excitation scheme and without the wall thickening effect. All three of the excitation schemes considered in this chapter produce physiologically plausible left ventricular volume changes with time.

4.3.2 Twist in the left ventricle

The second step in validating our model is to consider the twisting action of the left ventricle. To aid in estimation of twist we use the "twist indicator" shown in grey in figure 4.5: this is a piece of very

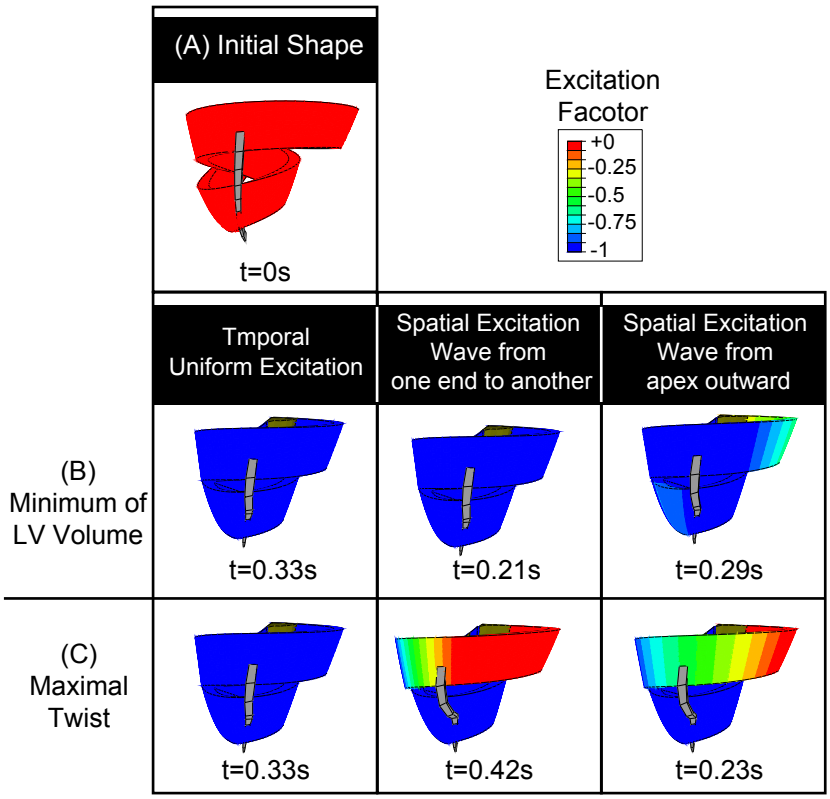

Figure 4.5: Snapshots of the movies for the adult heart model. The legend for the excitation factor is at the top right corner (red-relaxed, blue-contracted). For each type of excitation discussed in this chapter we show the snapshots of the band at the time at which left ventricular (B) volume was at a minimum and (C) the twist was at a maximum. The presence of twist can be qualitatively judged by the out of plane deformation of the grey twist indicator. For the uniform excitation, no out of plane movements can be qualitatively seen. The models subject to the spatial excitation have twist indicator deformations out of plane. To showcase this, we provide another series of snapshots for the spatial wave excitations for times at which the twist was maximal (bottom panels). (A) Initial shape at time, $t = 0s$. (B) Minimum volume: Uniform excitation at t=0.33s; Spatial excitation wave from one end of the band to the other at t=0.21s; Spatial excitation wave from apex at t=0.29s. (C) Maximal twist: Uniform excitation at t=0.33s; Spatial excitation wave from one end of the band to the other at t=0.42s; Spatial excitation wave from apex at t=0.23s.

soft material (100 times softer than collagen) which we computationally attached to the band; it is so soft that it does not affect the band dynamics, but its deformation, driven by the band, can be used to measure twist. Figure 4.5C shows qualitatively that the spatial (traveling) excitation wave causes greater twist than a temporal excitation scheme. Indeed, strongest twist in the cases of the spatial waves is close to physiological with absolute values of over 0.04 rad/cm, while the maximum of the absolute value of the twist in a uniform excitation is only 0.03 rad/cm. However, the main differentiation factor between the different excitation scheme is the timing of the minimum volume of the left ventricle relative to the timing of maximal twist.

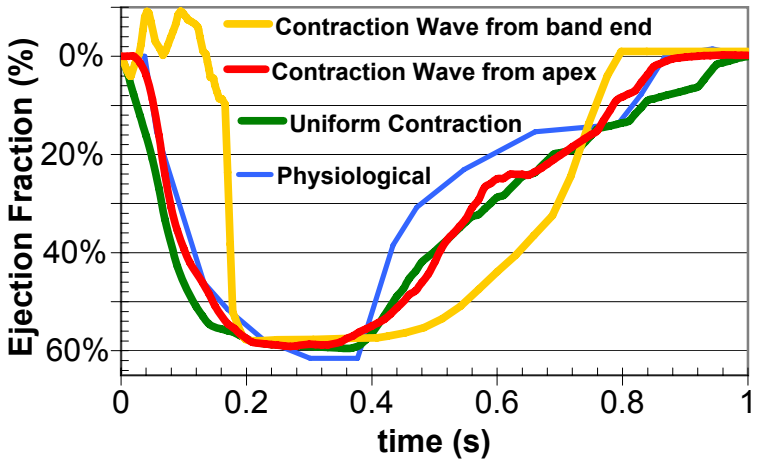

Figure 4.6: Ejection Fraction vs. Time for four cases: green - uniform (entire band contracting at once), time dependent contraction; yellow - a spatial wave contraction starting from the RH end of the band and traveling to the opposite end; red - a traveling Purkinje type spatial wave starting at the apex and moving outward; blue - physiological case adapted from Guyton and Hall [15]. The response to the time dependent contraction is piece-wise linear corresponding to the degree of excitation. The response to the simple (going from one end of the band to the other) spatial wave contraction presents an unphysiological initial increase in volume. The response to the Purkinje type spatial wave does a much better job at matching both the systolic and diastolic physiological behavior than the other spatial wave.

4.3.3 Timing relationship between twist and ejection fraction

We found that all of the trial excitation patterns are able to match the physiological ejection fraction. Additionally, the spatial excitation waves are able to induce physiologically large twist in the ventricle. But how are these correlated? The relationship between these two ventricular properties is important, as Miller [27] and others have observed that it is an important aspect of the volume efficiency. The best way to characterize this timing relationship between the twist of the left ventricle and the volume exchange dynamics is the parametric plot of twist against ejection fraction, parameterized by the time through the beat. We can imagine that a representation point moves on the plane of twist versus ejection fraction as the heart beat develops. In normal heart, this results in a peculiar double-looped shape, as indicated in figure 4.7A. The shape of this parametric representation is very sensitive to the damage in a myocardium [64].

In our simulations we show that only spatio-temporal excitation patterns give rise to a hysteresis-like double-loop relationship. In case of a uniform excitation the ventricle simply twists and untwists uniformly (figure 4.7B). As we follow the looped relationship between twist and ejection fraction for the model activated by a spatial wave starting at the pulmonary aorta and moving to the other end, we notice that we move through the loop in the reverse direction from the normal case (figure 4.7C). This means that instead of taking advantage of the potential energy stored during the contraction

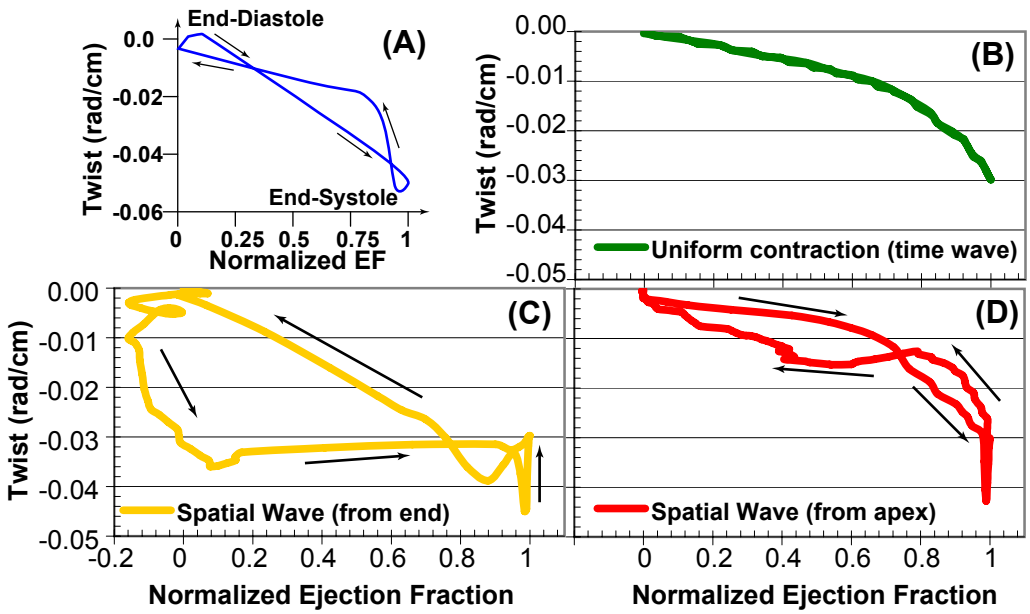

Figure 4.7: Plots of twist vs. normalized ejection fraction. The arrows indicate the progression direction with time. (A) A schematic representation of physiological results adapted from a paper by Moon et al. [27]. (B) Model results for uniform time dependent contraction. The ventricle simply twists and untwists along the same path. (C) Model results for simple spatial wave (traveling from one end to the other). While this presents a looped behavior, the arrows are in reverse of physiologically observed, which means the ventricle is working against the twist instead of utilizing it during the filling stages. (D) Model results for the Purkinje type wave. The relationship between twist and ejection fraction in this case is a physiological type double loop with the correct directions and the magnitude of the twist also matches experimental observations.

stage in the deformed material, the heart needs to perform extra work to overcome the twisting. Importantly, we conclude that the traveling contraction wave mimicking the Purkinje activation system is the one to reproduce the intricate relationship between twist and ejection fraction (figure 4.7D).

4.3.4 Varying the point of the initiation of spatial excitation waves

So far we have presented in detail the effect of two different spatial excitation waves: in one of them, the excitation wave starts at the pulmonary end of the band and travels to the other end; in another, the excitation starts in the middle of the band at the lowest point - the apex. It is possible, by varying the value of parameter AI, to create excitation schemes that lie in between of these two extremes, where the excitation starts neither at the end of the band nor at the apex. Additionally, by adjusting the speed of the excitation and relaxation wave fronts (adjusting constants U_i) the left ventricular volume changes can be made to closely match physiological. However, the relationship

between twist and ejection fraction is very sensitive to the location of the initial wave fronts. Indeed, if the wave fronts do not initiate in the inner loop, i.e., the septum and apex region, it does not seem to be possible to reproduce the double looped hysteresis. Therefore, we conclude that unless the excitation is initiated in the septum close to the apex, the refilling of the ventricle will not be efficient.

It is also possible to create excitation patterns that would move through the layers of the band, rather than only longitudinally along the band. This would provide a fine tune control of the timing of the twisting of the ventricle. Indeed, if the location of the initiation of excitation impacts each region of hysteresis loop, an ability of the signal to propagate through the layers could provide for control of the different parts of the loop. However, it is worth it to note here, that to an imaging technique incapable of resolving the muscle fibers from the myocardium wall the excitation wave that are modeled here would appear to move through the layers of the wall from the inner wall toward the outer.

4.4 Conclusion

By avoiding the complexity of modeling the whole heart structure at once, including all of the collagen and blood, we show that the double helical simple band structure is akin to an engine behind the heart pumping action. Indeed, by coupling this band-like structure of the myocardium with a Purkinje-type contraction scheme, we were able to achieve both the physiological ejection fraction of 60% and the important twisting pattern, without exceeding the contractile ability of the myofibrils. It is also possible to use this simple model to show the reduction in pumping efficiency when the main fiber orientation at the apex becomes more oblique, as happens after an infarction if the heart dilates in DCM. The model can also be used to model infarctions of different parts of the myocardium. Our results illustrate the dominance of the single-band structure, which can now be used to develop a new generation of heart models.